Polarons and excitons on a cylinder: a simplified model for nanotubes in polar environments

2007 J. Phys.: Condens. Matter 19 156210

(http://iopscience.iop.org/0953-8984/19/15/156210)

IOP PUBLISHING JOURNAL OF PHYSICS: CONDENSED MATTER

J. Phys.: Condens. Matter **19** (2007) 156210 (12pp) doi:10.1088/0953-8984/19/15/156210

Polarons and excitons on a cylinder: a simplified model for nanotubes in polar environments

Yu N Gartstein[1], **T D Bustamante**[1] **and S Ortega Castillo**[2]

[1] Department of Physics, The University of Texas at Dallas, PO Box 830688, FO23, Richardson, TX 75083, USA
[2] FAMAT, University of Guanajuato, Guanajuato, Mexico

Received 29 December 2006, in final form 28 February 2007
Published 21 March 2007
Online at stacks.iop.org/JPhysCM/19/156210

Abstract

Excess charge carriers on semiconducting nanotubes immersed in sluggish polar environments can undergo self-localization into polaronic states. Using a simplified model of electrons and holes of equal effective masses and confined to a cylindrical surface in the three-dimensional polar medium, we evaluate the binding energy E_b^{pol} of adiabatic Fröhlich–Pekar polarons and compare it to the corresponding exciton binding energy E_b^{exc}. The ratio E_b^{pol}/E_b^{exc} is found to be a non-monotonic function of the cylinder radius R which, in an idealized model, can reach values of about 0.35, substantially larger than values of about 0.2 for two-dimensional (2D) or three-dimensional (3D) systems. We argue that these findings represent a more general crossover effect that could manifest itself in other semiconductor nanostructures in 3D polar environments. As a result of the strong polaronic effect, the activation energy of exciton dissociation into polaron pairs is significantly reduced, which may lead to enhanced charge separation.

1. Introduction

Low-dimensional semiconductor structures such as quantum wells, quantum wires, nanotubes and conjugated polymers are important for practical applications and interesting scientifically. It is known that the confinement of the motion of charge carriers in some directions leads to increased effects of the Coulomb interaction on system excitations. In this paper we are concerned with two types of such effects: *excitonic* and *polaronic*. The excitonic effect refers to the formation of Coulombically bound electron–hole pairs, Wannier–Mott excitons, which progressively affect optical properties of semiconductors: the exciton binding energy E_b^{exc} increases from its 3D value to 2D and, further on, to quasi-one-dimensional (1D) magnitudes (E_b^{exc} diverges in pure 1D) [1]. The polaronic effect occurs in polar media, where the Coulomb field of an individual charge carrier causes the polarization (deformation) of its surroundings, resulting in the carrier self-localization into polaronic states. Such polarons have been extensively studied especially in the context of 3D ionic crystals and polar

semiconductors [2–5]. The polaronic effect also grows with the confinement: the polaron binding energy E_b^{pol} in 2D is larger than in 3D and would diverge in pure 1D [6, 7]. Multiple aspects of the excitonic and polaronic effects have been explored in many publications for various specific low-dimensional systems.

Of particular interest to us is a relationship between E_b^{exc} and E_b^{pol}, each of the binding energies understood as being measured from the band edges in the absence of the polaronic effect. The ratio E_b^{pol}/E_b^{exc} of the binding energies has a clear significance for the relative energetics of closely bound and well-separated electron–hole pairs that is expected to affect practically important processes of charge separation and recombination. The bare value E_b^{exc} signifies the ionization energy, whether thermal or photo, required for 'unbinding' of the exciton into a well-separated band-edge electron and hole. In the presence of the polaronic effect, however, the thermal ionization (dissociation) would occur into a distant electron–polaron and hole–polaron so that the exciton thermal ionization energy is reduced from E_b^{exc} to $E_b^{exc} - 2E_b^{pol}$. We are interested in how much of this relative reduction might be possible to achieve due to the formation of *strong-coupling* (adiabatic) polarons. Our discussion here is restricted to systems with equal electron and hole effective masses, $m_e = m_h = m$, so that the electron–polaron and hole–polaron have the same binding energies while the closely bound exciton is neutral both globally and locally and therefore does not polarize the sluggish component of the medium in the adiabatic approximation [8, 9].

It is instructive to look at the ratio E_b^{pol}/E_b^{exc} based on the results known for isotropic systems of 'well-defined' dimensionality, that is, for purely 3D, 2D and 1D systems. One would then find that, while each of the binding energies increases with more confinement, their growth occurs nearly 'in proportion' so that the ratio does not change significantly. Indeed, the classic Pekar's result [10] for 3D adiabatic polarons would translate into the maximum ratio of about 0.22. The exciton binding in 2D increases by a factor of four from its 3D value [1] but the polaron binding energy in 2D increases by almost as much [6], resulting in the ratio $\simeq$0.20. Moreover, if the divergent purely 1D binding energies are taken (parametrically) for their ratio, then the result of [7] would translate into a maximum E_b^{pol}/E_b^{exc} of approximately 0.17.

From the standpoint of this data, the results of our recent *model* quasi-1D calculations [11] for polarons and excitons on nanotubes immersed in a 3D polar medium, yielding E_b^{pol}/E_b^{exc} in excess of 0.3, appear quite surprising. In the particular case of the tubular geometry, charge carriers are confined to motion on a cylindrical surface. Our study [11] was restricted to relatively small cylinder radii R. In this paper we will use a direct variational approach to calculate adiabatic polarons for arbitrary R, thereby enabling an assessment of the evolution of the ratio E_b^{pol}/E_b^{exc} between the purely 2D ($R \to \infty$) and quasi-1D regimes. The corresponding calculations for excitons on a cylindrical surface have been performed recently [12, 13] and are very much in line with our exciton data. We will demonstrate explicitly (see figure 2(b)) that the ratio of the polaron and exciton binding energies exhibits non-monotonic behaviour as a function of the cylinder radius and can achieve values as large as about 0.35 at intermediate R, where the cylinder circumference is roughly comparable to an appropriate Bohr radius. We believe that our demonstration of E_b^{pol}/E_b^{exc} ratios above the values in purely 3D and 2D systems can be rationalized by invoking simple physical arguments. These arguments also suggest that the *relative* increase in the polaronic effect that is found may reflect a general behaviour that might be characterized as a crossover effect.

Consider a gradual increase in the confinement, e.g. by starting to decrease the radius of a very large cylinder in going from the purely 2D system towards quasi-1D or by starting to decrease the thickness of a very thick quantum well in going from the purely 3D system towards 2D. Stated simplistically, the spatial size (extent) of a still unconfined polaron wavefunction

is larger than that of an unconfined exciton. As the confinement increases, therefore, the polaron can start experiencing substantial growth in its binding energy due to the confinement before a 'proportionally' substantial growth of the exciton binding energy sets in. With yet further increase in confinement, both polaron and exciton binding energies will reflect fuller confinement effects, resulting in the corresponding trend of the decreasing ratio E_b^{pol}/E_b^{exc}. Of course, quantitative aspects of the evolution can vary for different systems and need to be evaluated accordingly. We also stress that the above consideration tacitly assumed the existence of a uniform 3D polarizable medium, with the confinement affecting *only* the motion of charge carriers. Strong violations of this assumption can significantly affect the outcome for the ratio of binding energies.

While serving as a suggestive illustration of possibly general behaviour, it is polarons and the relationship of polarons and excitons on a cylindrical surface that are the subjects of our direct interest in this paper. Organic and inorganic tubular (nano)structures (see, e.g., [14, 15]) attract a great deal of attention and are considered to be candidate systems for important applications like (photo)electrochemical energy conversion and the (photo)catalytic production and storage of hydrogen, as well as in optoelectronics. On the one hand, their extended size along the tube axis can facilitate very good electron transport in that direction. On the other hand, tubes can expose large areas of both exterior and interior surfaces to facilitate surface-dependent reactions. Many of these applications involve contact with polar liquid environments such as common aqueous and non-aqueous solvents and electrolytic solutions which can provide conditions appropriate for the strong polaronic effect [11], thereby changing the nature of charge carriers. A widely known example of the tubular geometry is single-walled carbon nanotubes (SWCNTs) and, in fact, redox chemistry of carbon nanotubes is an 'emerging field of nanoscience' [16]. We note that the importance of the excitonic effects in the optics of semiconducting SWCNTs is well established now, with binding energies E_b^{exc} experimentally measured in some SWCNTs to be in the range of 0.4–0.6 eV [17–19]. There is also growing evidence of environmental effects on the electronic properties of SWCNTs [20–22].

It can be anticipated that the polaronic effect that we discuss would have an influence on both charge-transfer reactions and charge carrier dynamics on the tubes. In the context of our discussion of the relative energetics, a substantial reduction in the activation energy due to the polaronic effect should be expected for electric-field-assisted exciton dissociation and charge separation on semiconducting nanotubes.

Our illustrative calculations of the polaronic effect in this paper do not take into account details of the electronic band structure and polarizability of different nanotubes but, instead, are restricted to a simplest model of electrons and holes confined to a cylindrical surface in the 3D dielectric medium. The assumption of equal electron and hole effective masses is a reasonable approximation, e.g. for SWCNTs as well as for boron nitride tubes [23].

2. Exciton and polaron energy functionals

As noted above, our basic model, following references [12] and [13], assumes that electron and hole are particles of the same effective mass m whose motion is restricted to the surface of the cylinder of radius R. The cylindrical surface itself is immersed in the uniform 3D dielectric continuum characterized, as is common in studies of the polaron [2–4] and solvation [24–26] effects, by two magnitudes of the dielectric permittivity: the high-frequency (optical) value of ϵ_∞ and the low-frequency (static) value of ϵ_s. In the case of liquid polar media, the slow component of the polarization is ordinarily associated with the orientational polarization of the solvent dipoles, and it is typical [25, 11] that $\epsilon_s \gg \epsilon_\infty$. The fast component of the polarization follows charge carriers instantaneously. The slow component of the polarization, on the other

hand, is considered to be static in the adiabatic picture to determine the electronic states; the slow component then responds to the averaged electronic charge distribution.

With $m_e = m_h$, there is no net charge density associated with the ground state of the neutral exciton that would cause a static polarization of the slow component ('non-polarizing exciton'). The Coulomb interaction between the electron and the hole in the exciton is screened only by the high-frequency dielectric response ϵ_∞ [8, 9, 27]. The total energy of the exciton as a function of the normalized wavefunction $\psi(\mathbf{r})$ of the electron–hole relative motion (reduced mass $m/2$) is then

$$\mathcal{E}^{\rm exc}\{\psi\} = K^{\rm exc} - U^{\rm exc} = \frac{\hbar^2}{m}\int d\mathbf{r}\ |\nabla\psi(\mathbf{r})|^2 - \frac{e^2}{\epsilon_\infty}\int d\mathbf{r}\,\frac{|\psi(\mathbf{r})|^2}{D(\mathbf{r})}, \tag{1}$$

whose global minimum determines the exciton ground-state wavefunction and its binding energy. For our geometry, position vector $\mathbf{r} = (x, y)$ is confined to the cylindrical surface, where we choose x to be along the cylinder axis and $-\pi R < y < \pi R$ to be along the circumferential direction; $|\nabla\psi(\mathbf{r})|^2 = (\partial\psi/\partial x)^2 + (\partial\psi/\partial y)^2$. Coulomb interaction is determined by the physical distance in the 3D space; in the flat geometry it would be $D(\mathbf{r}) = |\mathbf{r}|$, for the points on the cylindrical surface

$$D(\mathbf{r}) = \left(x^2 + 4R^2\sin^2\frac{y}{2R}\right)^{1/2}. \tag{2}$$

Optimization of the functional (1) for the ground state of the exciton on a cylinder has been performed in [12] and [13], with the results being in very good agreement with our data to be used in the comparison with the polaron.

The polarons that we discuss here are of the large-radius Fröhlich–Pekar type, where the Coulomb field of an individual charge carrier supports a self-consistent dielectric polarization pattern surrounding the carrier. The formation of large-radius polarons (self-localization, self-trapping) occurs due to the interaction of charge carriers with the 'slow' component of polarization. As the fast component of polarization does not contribute to the polaronic effect, it is the effective dielectric constant ϵ^*:

$$1/\epsilon^* = 1/\epsilon_\infty - 1/\epsilon_s, \tag{3}$$

which affects the coupling strength [2–4, 24–26]. In the adiabatic approximation, the normalized wavefunctions $\psi(\mathbf{r})$ of a self-localized charge carrier correspond to the minima of the following polaron energy functional:

$$\mathcal{E}^{\rm pol}\{\psi\} = K^{\rm pol} - U^{\rm pol} = \frac{\hbar^2}{2m}\int d\mathbf{r}\ |\nabla\psi(\mathbf{r})|^2 - \frac{e^2}{2\epsilon^*}\int d\mathbf{r}_1\, d\mathbf{r}_2\,\frac{|\psi(\mathbf{r}_1)|^2\ |\psi(\mathbf{r}_2)|^2}{D(\mathbf{r}_1 - \mathbf{r}_2)}, \tag{4}$$

whose global minimum we will be seeking for the ground state of the polaron. The functional (4) has the form that is well known for the large strong-coupling polarons [5, 9] and is a result of the optimization of the total adiabatic energy functional with respect to the polarization of the medium, thereby exhibiting an effective self-interaction of the electron [4, 9, 11]. Correspondingly, the $U^{\rm pol}$ term in equation (4) is known to be 'made of' two parts: $-U^{\rm pol} = -U^{\rm pol}_{\rm el} + U^{\rm pol}_{\rm d}$, where $U^{\rm pol}_{\rm el}$ represents the magnitude of the potential energy of the electron in the polarization field and $U^{\rm pol}_{\rm d}$ represents the energy required to create this polarization ('deformation energy'); with the optimal polarization, $U^{\rm pol}_{\rm d} = U^{\rm pol}_{\rm el}/2$.

Both energy functionals (1) and (4) assume that the electron and hole energies are measured from the band edges.

It is convenient to factor out dependences on physically relevant combinations of parameters by introducing appropriate units of energy and length. We will choose such units based on combinations for the exciton Bohr radius and binding energy (effective Rydberg) in 3D:

$$a_0 = 2\epsilon\hbar^2/me^2, \qquad \mathrm{Ryd} = e^2/2\epsilon a_0. \tag{5}$$

For the exciton problem, equation (1), one uses $\epsilon = \epsilon_\infty$ in equation (5), and for the polaron problem, equation (4), one uses $\epsilon = \epsilon^*$. We use superscript indices 'exc' and 'pol' to distinguish between the corresponding units (5). With all the coordinates (x, y for the cylinder) measured in appropriate a_0, one arrives at dimensionless energy functionals, $\mathcal{E}_0^{\mathrm{exc}} = \mathcal{E}^{\mathrm{exc}}/\mathrm{Ryd}^{\mathrm{exc}}$ and $\mathcal{E}_0^{\mathrm{pol}} = \mathcal{E}^{\mathrm{pol}}/\mathrm{Ryd}^{\mathrm{pol}}$, where

$$\mathcal{E}_0^{\mathrm{exc}}\{\psi\} = \int \mathrm{d}\mathbf{r}\ |\nabla\psi(\mathbf{r})|^2 - 2\int \mathrm{d}\mathbf{r}\,\frac{|\psi(\mathbf{r})|^2}{D_0(\mathbf{r})} \tag{6}$$

and

$$\mathcal{E}_0^{\mathrm{pol}}\{\psi\} = \frac{1}{2}\int \mathrm{d}\mathbf{r}\ |\nabla\psi(\mathbf{r})|^2 - \int \mathrm{d}\mathbf{r}_1\,\mathrm{d}\mathbf{r}_2\,\frac{|\psi(\mathbf{r}_1)|^2\ |\psi(\mathbf{r}_2)|^2}{D_0(\mathbf{r}_1-\mathbf{r}_2)}. \tag{7}$$

The dimensionless $D_0(\mathbf{r})$ in equations (6) and (7) features the same behaviour as equation (2) but with R replaced by the corresponding $R_0 = R/a_0$.

The global minima of equations (6) and (7), $-E_0^{\mathrm{exc}}$ and $-E_0^{\mathrm{pol}}$ respectively, would determine the dimensionless binding energies. As the units (5) already establish the scaling rules, in what follows we will be comparing E_0^{exc} and E_0^{pol} at the same values of R_0. The ratio $E_0^{\mathrm{pol}}/E_0^{\mathrm{exc}}$ would have a direct physical meaning of the maximum achievable when $\epsilon_{\mathrm{s}} \gg \epsilon_\infty$ and $\epsilon^* \simeq \epsilon_\infty$ in equation (3). As we mentioned earlier, this can be a typical situation for many polar solvents.

Before proceeding with the analysis for a cylindrical surface, we recall in more detail the benchmarks known for isotropic d-dimensional systems ($D_0(\mathbf{r}) = |\mathbf{r}| = r$) briefly described in the introduction. The exact isotropic excitonic ground state $\psi(r)$ corresponding to equation (6) is given by the solution of the Schrödinger equation,

$$-E_0^{\mathrm{exc}}\psi = -\frac{\partial^2\psi}{\partial r^2} - \frac{(d-1)}{r}\frac{\partial\psi}{\partial r} - \frac{2}{r}\psi,$$

yielding well-known

$$\psi(r) \propto \exp\left(-\frac{2r}{d-1}\right), \qquad E_0^{\mathrm{exc}} = \frac{4}{(d-1)^2}. \tag{8}$$

With our choice of units, $E_0^{\mathrm{exc}} = 1$ in 3D.

The polaronic ground-sate wavefunctions and energies corresponding to equation (7) are known from variational calculations for d-dimensional systems. It is customary in the polaronic literature to express energies in terms of the coupling constant $\alpha_{\mathrm{c}} = \left(me^4/2\epsilon^{*2}\hbar^3\omega\right)^{1/2}$ and phonon frequency ω. Note that the combination $\alpha_{\mathrm{c}}^2\,\hbar\omega$ appearing in the results for strong-coupling (adiabatic) polarons corresponds to $2\mathrm{Ryd}^{\mathrm{pol}}$, as defined in equation (5). Thus the well-known Pekar's result [10] for the 3D polaron translates into $E_0^{\mathrm{pol}} \simeq 0.218$ and into the same magnitude of the ratio $E_0^{\mathrm{pol}}/E_0^{\mathrm{exc}}$ in 3D.

The 2D polaron has been studied in great detail in [6], with the best result of $E_0^{\mathrm{pol}} \simeq 0.809$ for the adiabatic case being achieved with Pekar-type trial wavefunctions. Since $E_0^{\mathrm{exc}} = 4$ in 2D, the ratio $E_0^{\mathrm{pol}}/E_0^{\mathrm{exc}} \simeq 0.202$, which is only slightly smaller than in 3D. The 2D case represents the limit $R \to \infty$ for a cylindrical surface and is particularly important for our

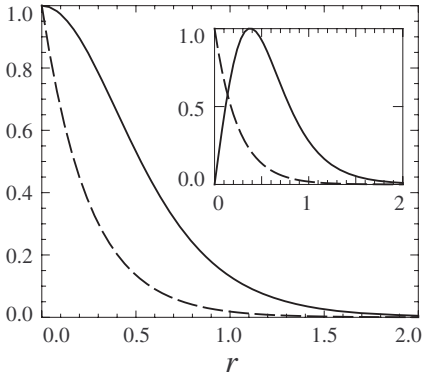

Figure 1. The spatial distribution of unnormalized density $|\psi(r)|^2$ for the exciton (dashed line) and the polaron (solid line) in 2D. The polaron wavefunction is as per equation (9). The inset shows the corresponding spatial distribution $U(r)$ of the potential energy in $U = \int U(r)\,\mathrm{d}r$.

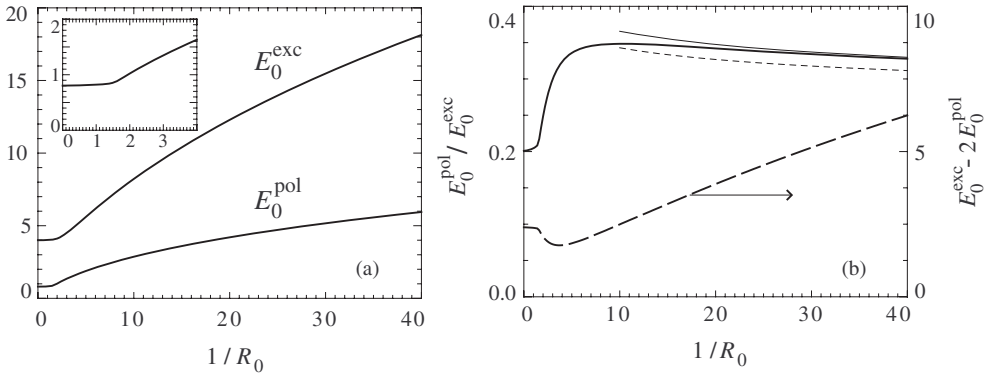

Figure 2. (a) The dimensionless exciton and polaron binding energies as functions of the dimensionless inverse cylinder radius $1/R_0$. The inset shows the behaviour of the polaron binding energy in more detail at small $1/R_0$. (b) The ratio of the binding energies $E_0^{\mathrm{pol}}/E_0^{\mathrm{exc}}$ of the excitations on a cylinder is shown as a thick solid line. A thin solid line displays this ratio as is obtained in the quasi-1D calculation with the effective tube potential (15). A thin short-dash line shows the quasi-1D result for this ratio if the effective interaction, instead, was that of a quantum wire, equation (16). A thick long-dash line displays the dimensionless activation energy $E_0^{\mathrm{exc}} - 2E_0^{\mathrm{pol}}$.

analysis. We have looked at simpler one-parametric trial wavefunctions that would make a good representation of the 2D adiabatic polaron and found that the wavefunction

$$\psi(r) \propto \frac{1}{\cosh(\alpha r)} \tag{9}$$

with $\alpha \simeq 1.674$ yields a very good optimization for the energy: $E_0^{\mathrm{pol}} \simeq 0.804$, which is quite accurate for our purposes. Figure 1 compares the spatial structure of the 2D exciton and polaron.

As both exciton and polaron binding energies diverge in pure 1D, the following comparison might be of a dubious nature but is still interesting. Specifically, reference [7] discussed the calculation of the 1D polaron in terms of the renormalized coupling constant $\alpha_{\mathrm{c}}' = \alpha_{\mathrm{c}}/(d-1)$, where $d \to 1$. The best variational result achieved for the adiabatic polaron was $E_{\mathrm{b}}^{\mathrm{pol}} \simeq$

$0.333\,(\alpha_c'^2\hbar\omega)$. As the diverging d-dependence in this expression is the same $(d-1)^{-2}$ as in the exciton case (8), the ratio of the binding energies in 1D could then be interpreted as $E_0^{\rm pol}/E_0^{\rm exc} \simeq 0.167$.

3. Variational analysis for a cylinder

When on a cylindrical surface, both exciton and polaron ground states need to be determined numerically. Our variational analysis of the energy functionals (6) and (7) has been performed on the following classes of the trial wavefunctions[3]. For the exciton problem we have used three-parametric (α, β and γ) wavefunctions

$$\psi(x, y) \propto \exp\left[-\left(\alpha^2 x^2 + \beta^2 y_1^2 + \gamma^2\right)^{1/2}\right]. \tag{10}$$

The polaron problem is much more demanding on computation time, so we chose two-parametric (α and β) wavefunctions

$$\psi(x, y) \propto \frac{1}{\cosh\left(\alpha^2 x^2 + \beta^2 y_1^2\right)^{1/2}}. \tag{11}$$

The functional dependences in equations (10) and (11) are such that they can recover, in the limit of $R_0 \to \infty$, wavefunctions (8) and (9) found for the 2D systems—similarly to the earlier exciton calculations [12, 13].

We explored two choices for the effective coordinate y_1 in equations (10) and (11): 'arc-based' (as in [13])

$$y_1 = y, \tag{12}$$

$-\pi R_0 < y < \pi R_0$, and 'chord-based' (as in [12])

$$y_1 = 2R_0 \sin\left(y/2R_0\right). \tag{13}$$

Both choices can be thought of as, respectively, $n \gg 1$ and $n = 1$ limits of more general

$$y_1 = \pi R_0 \left\{\frac{2}{\pi}\sin\left[\frac{\pi}{2}\left(\frac{y}{\pi R_0}\right)^n\right]\right\}^{1/n}$$

which could be used in future refinements as being more flexible in terms of the shape of the wavefunction being periodic in the circumferential direction. In this paper we resorted to just choosing the best results among those obtained with equations (12) and (13).

Wavefunctions (10) and (11) feature two parameters α and β having the meaning of inverse lengths, thereby explicitly allowing for anisotropy of the wavefunction extent in the axial and circumferential directions [13]. What we will later be referring to as quasi-1D results corresponds to $\beta = 0$ when the wavefunctions are uniform around the cylinder circumference.

The main quantitative results of this paper are displayed in figure 2, showing the optimized variational outputs for the exciton and polaron binding energies as well as their ratio $E_0^{\rm pol}/E_0^{\rm exc}$. Our exciton data is very close to the results of [12] and [13], where the reader can find extensive discussions.

Just as in the exciton case, the polaron binding energy exhibits very little change from its 2D value ($\simeq$0.8) due to the curvature of up to $R_0 \sim 1$ (see the inset in figure 2(a)) where it starts rising, relatively earlier and more rapidly than the exciton dependence. This immediately translates into a substantial increase in the ratio $E_0^{\rm pol}/E_0^{\rm exc}$ with decreasing R_0, as shown in figure 2(b). The maximum of the ratio $\simeq$0.35 is achieved in the region of $1/R_0 \sim 10$, after

[3] All numerical integrations and optimizations have been performed by using IMSL numerical libraries, as provided with the PV-WAVE Advantage package, http://www.vni.com.

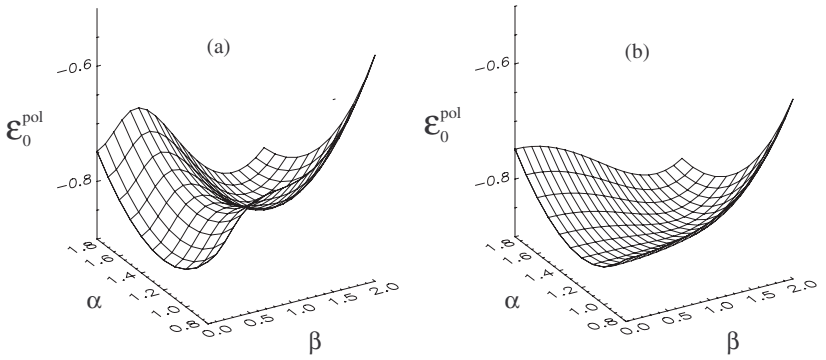

Figure 3. The behaviour of the functional (7) at $R_0 = 0.65$ with the trial wavefunctions (11) as a function of the variational parameters α and β for two choices of the effective coordinate y_1: (a) as in equation (12) and (b) as in equation (13).

which the ratio starts slowly decreasing with $1/R_0$. While, of course, larger ratios $E_0^{\rm pol}/E_0^{\rm exc}$ lead to larger relative reductions in the effective activation energy $E_0^{\rm exc} - 2E_0^{\rm pol}$, it is quite interesting that the *absolute* value of this activation energy, also shown in figure 2(b), exhibits a non-monotonic dependence on $1/R_0$. A region around the minimum of this curve indicates specific tube sizes where the activation energy would be at its lowest.

Our variational results have shown that the the dependence of $E_0^{\rm pol}$ on $1/R_0$ collapses onto the corresponding quasi-1D curve practically right away after the onset of a substantial rise in binding. This is different from the exciton case, where deviations from the quasi-1D behaviour persist all the way into the region of $1/R_0 > 20$. In other words, the polaron spreads uniformly around the cylinder at much smaller curvatures than the exciton does. We note that the quasi-1D variational results for the polaron binding using trial wavefunctions (11) and (10) differ very little and are in good agreement with our analysis in [11], where no assumptions have been made about the wavefunction shape and the nonlinear optimizing equation has been solved numerically. The thin solid line in figure 2(b) shows the ratio $E_0^{\rm pol}/E_0^{\rm exc}$ using quasi-1D results for the binding energies, and its deviation from the variational result for a cylinder is entirely due to underestimation of the exciton binding.

As with all variational calculations, we, of course, cannot exclude that some details in the results shown in figure 2 may undergo slight modifications upon further improvements of variational wavefunctions. Importantly, possible improvements would be inconsequential for our main observations of a non-monotonic dependence of the ratio $E_0^{\rm pol}/E_0^{\rm exc}$ on $1/R_0$ and of the magnitude of the ratio reaching values well above the 2D value of $\simeq$0.2. We found that a rise in the ratio above 0.3 is obtainable even if the polaron wavefunctions are not specifically optimized for a range of given R_0 but the 2D optimal values of $\alpha = \beta \simeq 1.67$ are used. For very small tubes with $1/R_0 < 20$, the results of exact numerical calculations in [11] complement the picture.

The transitional region of $R_0 \sim 1$ is likely to be especially sensitive to the choice of trial wavefunctions. So, reference [12] reported an improvement of a few percent for the exciton binding energy in the region of $1 < 1/R_0 < 2.5$ with certain trial functions. Similar improvements could perhaps be found for the polaron binding energies. Figure 3 illustrates the behaviour of the polaron functional (7) in the transitional region, at $R_0 = 0.65$, as a function of the variational parameters α and β. A curious feature of the 'landscape' in figure 3(a) is a clear coexistence of two minima, one corresponding to a polaronic state that

is uniformly distributed (delocalized) around the cylinder circumference, and the other where the circumferential distribution is non-uniform. While this appears as an interesting possibility, it could also be an artefact of a restricted nature of a specific class of the trial wavefunctions; compare visually, for example, to the landscape of figure 3(b). A much more careful study would be needed to explore the possibility of coexisting polaronic states requiring an analysis of actual adiabatic potential surfaces. An example of an analogous analysis can be found in [28], where we proved a coexistence of different polarons in certain quasi-1D systems.

4. Discussion

Both in this paper and in [11] we have shown that the strong polaronic effect occurring in sluggish polar environments substantially affects the relative energetics of closely bound and well-separated electron–hole pairs on a cylindrical surface of nanotubes. The binding energy $E_{\rm b}^{\rm pol}$ of an individual polaron can, in an idealized model, reach as much as about 0.35 of the binding energy $E_{\rm b}^{\rm exc}$ of the exciton. This would translate into a reduction in the activation energy $E_{\rm b}^{\rm exc} - 2E_{\rm b}^{\rm pol}$ for exciton dissociation by a factor of about three from the value $E_{\rm b}^{\rm exc}$ that it would have in a non-polar environment with the same value of the high-frequency dielectric constant ϵ_∞. Note that, in our earlier study [11], we have not found any additional energy barriers between the exciton and distant polaron-pair states. One should expect that enhanced separation of charges and a corresponding luminescence quenching would then result, for example, in experiments probing the effects of electric field on the luminescence. It is needless to say that additional factors omitted in our simplified analysis here can make the reduction magnitude smaller (see, e.g., a comparison in [11] of cases with different 'electrostatic conditions').

Polar liquid environments such as many common solvents may be good candidates for providing conditions necessary for the strong polaronic effect, as they can exhibit both high values of the static dielectric constant $\epsilon_{\rm s}$ and a relatively slow response of the orientational polarization (longitudinal relaxation times can be on the order of 1 ps and longer) [25, 11]. Quite fittingly, there is an ongoing intense research effort on various applications of nanotubes in contact with such environments, and we hope that direct experimental verifications of our qualitative conclusions will be possible. We note that a comprehensive mapping of luminescence versus absorption spectra of individual SWCNTs was in fact achieved in aqueous suspensions [29, 30]. Interestingly, numerical estimates in [13] indicate that the dimensionless radius R_0 for a range of SWCNTs may be close to 0.1, which corresponds to the region of maximum $E_0^{\rm pol}/E_0^{\rm exc}$ ratios in figure 2(b).

We have demonstrated that the ratio of the binding energies $E_{\rm b}^{\rm pol}/E_{\rm b}^{\rm exc}$ has a non-monotonic dependence on the cylinder curvature $1/R$. As argued in the introduction, our particular observation for the cylindrical geometry can be a manifestation of a more general crossover effect that would be common for other structures in 3D polar media when the increasing confinement of the electron motion causes a 'transition' between d-dimensional systems, such as between 3D and 2D (quantum wells) or between 3D and 1D (quantum wires). Basically, the origin of this effect can be related to the fact that the spatial extent of an unconfined polaron is larger than the size of an unconfined exciton (see figure 1 for the 2D case), thereby making the polaron 'respond' to the initially increasing confinement in a more pronounced way than the exciton. Only after the exciton experiences a fuller effect of the confinement, the ratio of the binding energies starts decreasing. Elaborating more on this idea, the inset in figure 1 shows the spatial distribution of the potential energy terms U: $\mathcal{E} = K - U$, for unconfined excitations. It is evident that the 'longer-range' contributions to the polaron potential energy are relatively more important than for the exciton. This is why the effect of increasing confinement on the

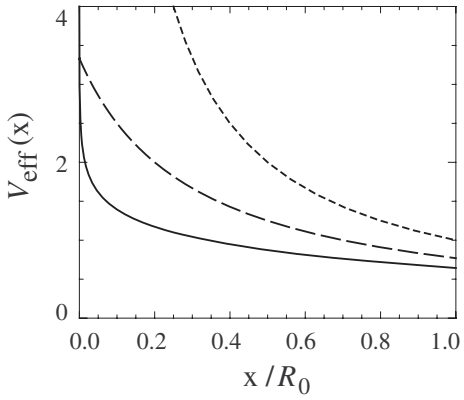

Figure 4. Distance dependence of the effective 1D Coulomb potentials for charges on a cylinder, equation (15), solid line, and in a quantum wire, equation (16), long-dash line, in comparison with the original Coulomb interaction (14), short-dash line.

polaron is initially stronger. In the particular case of the cylindrical geometry, the curvature changes remote physical distances (chords instead of arcs, equation (2)) more than it does close distances.

A meaningful parallel can be drawn with the behaviour of the ratio U/K of the potential and kinetic energy terms in confined systems. The virial theorem for the Coulombically bound states in unconfined d-dimensional systems states that $U/K = 2$, independent of d, which, of course, also follows directly from scaling of both functionals (1) and (4) provided that $D(\mathbf{r}) = |\mathbf{r}| = r$. In particular, polarons in such systems are known [31, 9, 4] to satisfy the following ratios for various energy terms: $E_{\rm b}^{\rm pol}$:$K^{\rm pol}$:$U^{\rm pol}$:$U_{\rm el}^{\rm pol}$:$U_{\rm d}^{\rm pol}$ = 1:1:2:4:2. Some of these relationships are violated in confined systems. As studied in [32], the virial theorem ratio $U^{\rm exc}/K^{\rm exc}$ for excitons in quantum wells and quantum wires is larger than 2 and, in fact, a non-monotonic dependence of $U^{\rm exc}/K^{\rm exc}$ has been demonstrated for quantum wells transitioning between 3D and 2D limits. We have found a non-monotonic behaviour of the ratio U/K for both polarons and excitons on a cylinder as a function of the curvature $1/R$. In agreement with our qualitative arguments, at smaller $1/R$ this ratio grows much more quickly for the polaron than for the exciton. At large curvatures, however, the trend is reversed and the exciton has larger ratios U/K than the polaron.

It is useful to continue a qualitative reasoning by discussing the quasi-1D limit of our results, that is, the case of stronger but still finite degrees of confinement. One can then use the notion of the effective Coulomb potentials [1, 32], here as a function of the 1D (axial) distance x. (The effective Coulomb potentials for 2D can be similarly introduced [32]). Figure 4 compares three potentials in units such that, at very large distances, the potentials behave as

$$V_{\rm eff}(x) = R_0/x. \tag{14}$$

In this limit the electron wavefunction on a cylinder is delocalized around its circumference and the effective interaction becomes that of rings of charge given by

$$V_{\rm eff}(x) = \frac{2}{\pi\left[(x/R_0)^2+4\right]^{1/2}} K\left[\frac{4}{(x/R_0)^2+4}\right], \tag{15}$$

where $K(m) = \int_0^{\pi/2}(1 - m\sin^2\theta)^{-1/2}\,{\rm d}\theta$ is a complete elliptic integral of the first kind. If, instead of a tube, we dealt with a quantum wire, the electron wavefunction would be delocalized

throughout the cross-section of the wire, with the effective interaction approximated as [1]

$$V_{\rm eff}(x) = \frac{1}{(x/R_0) + 0.3}. \tag{16}$$

Both effective tube (15) and wire (16) 1D potentials feature modifications of the shorter-range interaction from the original Coulomb (14) due to the transverse spread of wavefunctions, thereby eliminating a pure 1D divergence of the ground states for excitons and polarons. As we discussed above, the role of the longer-distance interactions is more important for the polaron than for the exciton. Since the relative modification of the original Coulomb to the effective potentials is increasing towards shorter distances, it is then clear that the ratio $E_{\rm b}^{\rm pol}/E_{\rm b}^{\rm exc}$ in systems with modified interactions should be larger than values of about 0.2 in systems with pure Coulomb interaction. Moreover, following the same logic, one should expect that the larger modification is from the original Coulomb distance dependence, the larger will be the $E_{\rm b}^{\rm pol}/E_{\rm b}^{\rm exc}$ ratios. Figure 4 shows that deviations from the Coulomb dependence for the effective wire potential are smaller than for the tube potential (over a relevant spatial range). We have performed a quasi-1D variational optimization of the polaron and exciton binding energies with the wire potential (16). The resulting ratios, $E_0^{\rm pol}/E_0^{\rm exc}$, are shown in figure 2(b) with a short-dash thin line and are, indeed, smaller than the ratios calculated with the tube potential (15)—solid thin line in that figure.

These qualitative arguments, while confirmed by specific model calculations, do not appear to be restricted to this specific situation. We therefore expect that findings of larger magnitudes of the ratio $E_{\rm b}^{\rm pol}/E_{\rm b}^{\rm exc}$ and of a non-monotonic dependence of this ratio on the degree of confinement represent a crossover effect that can be common to semiconductor nanostructures in 3D polar environments. Further calculations with different geometric structures are needed to validate this conjecture and evaluate its quantitative aspects, including in non-uniform polar environments.

We would like to reiterate that numerical data that we arrived at in this paper are based on a simplified model; more accurate calculations would have to take into account specific aspects of the nanotube band structure and the tube's own polarizability. Optical studies of SWCNTs particularly indicate the dependence of the exciton binding not only on R but also on the chirality of the tubes; see the discussion and multiple citations in [33]. The latter reference also shows separately the effect on excitons of tube's polarizability; our earlier quasi-1D calculations are consistent with their findings, and we refer the reader to [11] for illustrations of this effect on polarons.

Another interesting subject for future research is an assessment of the activation energy for exciton dissociation in confined semiconductors with unequal electron and hole masses, $m_{\rm e} \neq m_{\rm h}$. In this case, electron–polarons and hole–polarons have different binding energies and, in addition, the exciton itself can cause an adiabatic polarization of the environment [8, 27]. The corresponding 'polaronic' corrections to the exciton binding in quantum-well wires have been studied, for example, in [34]. From a general standpoint, one would also like to extend the analysis of the effects of polar media on the dissociation of confined excitons to the intermediate-coupling [2–4] regime.

Acknowledgments

We are deeply grateful to V M Agranovich for many useful discussions. This study was supported by the Collaborative University of Texas at Dallas–SPRING Research and Nanotechnology Transfer Program. The work of SOC was supported by the University of Texas at Dallas Summer Research Program.

References

[1] Haug H and Koch S W 2004 *Quantum Theory of the Optical and Electronic Properties of Semiconductors* (New Jersey: World Scientific)
[2] Fröhlich H 1954 *Adv. Phys.* **3** 325
[3] Kuper C G and Whitfield G D (ed) 1963 *Polarons and Excitons* (New York: Plenum)
[4] Appel J 1968 *Solid State Physics* vol 21, ed F Seitz, D Turnbull and H Ehrenreich (New York: Academic) p 193
[5] Alexandrov A S and Mott N 1995 *Polarons and Bipolarons* (Singapore: World Scientific)
[6] Wu X, Peeters F M and Devreese J T 1985 *Phys. Rev.* B **31** 3420
[7] Peeters F M and Smondyrev M A 1991 *Phys. Rev.* B **43** 4920
[8] Dykman I M and Pekar S I 1952 *Dokl. Akad. Nauk SSSR* **83** 825
[9] Rashba E I 1987 *Excitons, Selected Chapters* ed E I Rashba and M D Sturge (Amsterdam: North Holland) p 273
[10] Pekar S I 1946 *Zh. Eksp. Teor. Fiz.* **16** 335
Pekar S I 1946 *Zh. Eksp. Teor. Fiz.* **16** 341
[11] Gartstein Yu N 2006 *Phys. Lett.* A **349** 377
[12] Kostov M K, Cole M W and Mahan G D 2002 *Phys. Rev.* B **66** 075407
[13] Pedersen T G 2003 *Phys. Rev.* B **67** 073401
[14] Tenne R 2002 *Semiconductor Electrodes and Photoelectrochemistry* ed S Licht (Weinheim: Wiley–VCH) p 238
[15] Zhao X S, Bao X Y, Guo W and Lee F Y 2006 *Mater. Today* **9** 32
[16] O'Connell M J, Eibergen E E and Doorn S K 2005 *Nat. Mater.* **4** 412
[17] Wang F, Dukovic G, Brus L E and Heinz T F 2005 *Science* **308** 838
[18] Ma Y-Z, Valkunas L, Bachilo S M and Fleming G R 2005 *J. Phys. Chem.* B **109** 15671
[19] Wang Z, Pedrosa H, Krauss T and Rothberg L 2006 *Phys. Rev. Lett.* **96** 047403
[20] Fantini C, Jorio A, Souza M, Strano M S, Dresselhaus M S and Pimenta M A 2004 *Phys. Rev. Lett.* **93** 147406
[21] Hertel T, Hagen A, Talalaev V, Arnold K, Hennrich F, Kappes M, Rosenthal S, McBride J, Ulbricht H and Flahaut E 2005 *Nano Lett.* **5** 511
[22] Lu M P, Hsiao C Y, Lo P Y, Wei J H, Yang Y S and Chen M J 2006 *Appl. Phys. Lett.* **88** 053114
[23] Mele E J and Král P 2002 *Phys. Rev. Lett.* **88** 056803
[24] Kuznetsov A M and Ulstrup J 1999 *Electron Transfer in Chemistry and Biology* (Chichester: Wiley)
[25] Fawcett W R 2004 *Liquids, Solutions and Interfaces* (Oxford: Oxford University Press)
[26] Nitzan A 2006 *Chemical Dynamics in Condensed Phases* (New York: Oxford University Press)
[27] Pekar S I, Rashba E I and Sheka V I 1979 *Sov. Phys.—JETP* **49** 129
[28] Gartstein Yu N and Zakhidov A A 1986 *Solid State Commun.* **60** 105
[29] O'Connell M J, Bachilo S M, Huffman C B, Moore V C, Strano M S, Haroz E H, Rialon K L, Boul P J, Noon W H, Kittrell C, Ma J, Hauge R H, Weisman R B and Smalley R E 2002 *Science* **297** 593
[30] Weisman R B, Bachilo S M and Tsyboulski D 2004 *Appl. Phys.* A **78** 1111
[31] Pekar S I 1951 *Research in the Electron Theory of Crystals* (Moscow: Gostekhizdat)
[32] Zhang Y and Mascarenhas A 1999 *Phys. Rev.* B **59** 2040
[33] Jiang J, Saito R, Samsonidze Ge G, Jorio A, Chou S G, Dresslhaus G and Dresslhaus M S 2007 *Phys. Rev.* B **75** 035407
[34] Degani M H and Hipólito O 1987 *Phys. Rev.* B **35** 9345